

UC Davis

UC Davis Previously Published Works

Title

Multi-objective optimisation for battery electric vehicle powertrain topologies

Permalink

<https://escholarship.org/uc/item/16x9d67d>

Journal

Proceedings of the Institution of Mechanical Engineers Part D Journal of Automobile Engineering, 231(8)

ISSN

0954-4070

Authors

Othaganont, Pongpun

Assadian, Francis

Auger, Daniel J

Publication Date


2017-07-01

DOI

10.1177/0954407016671275

Peer reviewed

Multi-objective optimisation for battery electric vehicle powertrain topologies

Proc IMechE Part D:
J Automobile Engineering
1–20
© IMechE 2016
Reprints and permissions:
sagepub.co.uk/journalsPermissions.nav
DOI: 10.1177/0954407016671275
pid.sagepub.com


Pongpun Othaganont¹, Francis Assadian² and Daniel J Auger¹

Abstract

Electric vehicles are becoming more popular in the market. To be competitive, manufacturers need to produce vehicles with a low energy consumption, a good range and an acceptable driving performance. These are dependent on the choice of components and the topology in which they are used. In a conventional gasoline vehicle, the powertrain topology is constrained to a few well-understood layouts; these typically consist of a single engine driving one axle or both axles through a multi-ratio gearbox. With electric vehicles, there is more flexibility, and the design space is relatively unexplored. In this paper, we evaluate several different topologies as follows: a traditional topology using a single electric motor driving a single axle with a fixed gear ratio; a topology using separate motors for the front axle and the rear axle, each with its own fixed gear ratio; a topology using in-wheel motors on a single axle; a four-wheel-drive topology using in-wheel motors on both axes. Multi-objective optimisation techniques are used to find the optimal component sizing for a given requirement set and to investigate the trade-offs between the energy consumption, the powertrain cost and the acceleration performance. The paper concludes with a discussion of the relative merits of the different topologies and their applicability to real-world passenger cars.

Keywords

Battery electric vehicles, multi-objective optimisation, powertrain topologies

Date received: 16 March 2016; accepted: 23 August 2016

Introduction

In recent years, environmental concerns have led many industries to focus on and to adopt green products and services. A good example of this is the passenger car, which is generally accepted as a major source of greenhouse gas emissions and air pollution. Governments have introduced legislation, taxation regimes and incentive schemes that force automotive companies to control vehicle emissions¹ and to encourage consumers to use efficient low-carbon vehicles. In the UK, for example, the government has subsidised 25% of the purchase price for ultra-low-emission cars since early 2012.² In response to all this, many automotive companies have attempted to reduce their fleet-averaged vehicle emissions by developing hybrid and electric vehicles.

Hybrid electric vehicles (HEVs) represent relatively mature technology and are readily available and affordable at the present time. Hybrid vehicles use two or more energy sources, with the intent of exploiting the advantages of each. As the most widespread form of a hybrid vehicle, HEVs combine the conventional

internal-combustion engine (ICE) with electric machines. The key advantage of this type of vehicle is that its fuel efficiency is greater than that of the conventional ICE vehicle; this results from the ability to downsize the engine and to operate it nearer to optimal conditions and, in some driving conditions, the ability to recover kinetic energy during braking. On the assumption of a diesel hybrid electric powertrain, one study has noted that a shift in the operating point caused by downsizing has the potential to reduce the overall fuel consumption by as much as 35% and that regenerative braking has the potential to provide a

¹Advanced Vehicle Engineering Centre, Cranfield University, Cranfield, Bedfordshire, UK

²Mechanical and Aerospace Engineering, University of California, Davis, California, USA

Corresponding author:

Daniel J Auger, Advanced Vehicle Engineering Centre, Cranfield University, School of Aerospace, Transport and Manufacturing, Building 115, College Road, Cranfield, Bedfordshire MK43 0AL, UK.
Email: d.j.auger@cranfield.ac.uk

further 8% reduction (see section 3.3.4 of the textbook by Guzzella and Sciarretta³). There are many results in the literature. For example, one extended study showed that, even without downsizing the engine, an operating point shift alone can produce a fuel savings of almost 30% in the New European Driving Cycle (NEDC)⁴ and over 20% in experimental tests and real-world driving cycles.⁵ Energy management systems continue to be a popular subject of research.

The HEV still derives its energy from fossil fuels and therefore still produces some pollution when driving on city roads. Ideally, a passenger car should use pure electric energy and produce zero tailpipe emissions. If a significant portion of the electricity can be generated from renewable sources, there is potential for further reductions in the true 'well-to-wheel' carbon emissions. One solution is the battery electric vehicle (BEV). There are others (such as the plug-in HEV and the fuel-cell electric vehicle) but the BEV is the fundamental base for these.

BEVs have been seen as a niche product, but they are now establishing themselves in the mainstream market. Several automobile companies have included a BEV in their range; examples include the Nissan LEAF in the UK and USA, the Tesla Roadster in the USA and the Mini E in Germany.^{6, 7} BEVs are well suited to everyday use since their battery capacity is sufficient for the day-to-day needs of many consumers. Pearre et al.⁸ reported that the majority of US drivers covered a daily mileage of less than 100 miles, comparing well with the daily mileage capacity of the vehicles in the current market.

The typical BEV in today's market differs from an ICE vehicle in that, instead of having an engine and a fuel tank, the BEV has an electric machine and an electric energy storage unit.^{9, 10} However, much of the rest of the vehicle is similar to a conventional vehicle; most BEVs still use a relatively conventional transmission system, including a clutch, a shaft drive, a gearbox and a differential. As with an ICE, the transmission affects the overall efficiency and the vehicle mass.¹⁰ Electric machines have rather different characteristics from those of ICEs; the typical electric machine provides its maximum torque at a low speed, in comparison with an ICE's peak torque at a particular speed. Consequently, electric vehicles can be operated with a single-ratio or double-ratio transmission⁹ rather than the five-or-more-speed transmission found in an ICE vehicle. The machines in today's market use various machine types (the Tesla Roadster and the Mini E use single induction motors while the Nissan LEAF uses a permanent-magnet synchronised motor), but all three use single-speed transmissions.^{6, 7} Apart from the number of gear ratios, the transmission in the typical BEV is very similar to that of the conventional ICE vehicle.

With a BEV, the designer is not constrained to using the traditional powertrain layout; there are several alternatives that are impossible or impractical with an ICE vehicle but are straightforward with an electric

powertrain. Rather than using a differential, it is possible to use an independent wheel drive, as discussed in the literature¹¹ and implemented in prototype cars; the Lightning GT uses a rear-wheel drive from twin traction motors, each with a single-speed reduction gearbox.¹² By using multiple machines, mechanical parts such as the differential can be eliminated and replaced by a 'virtual' differential effect from electrical control. It is also possible to transfer energy 'by wire' and to locate electric machines close to their point of action, eliminating large mechanical transmission components; as well as reducing the mass and adding flexibility, this can simplify the mechanical layout and reduce the space requirements. There are disadvantages; if an independent wheel drive is used, great care needs to be taken to design the complex non-linear control laws needed for stability and safety. With a conventional vehicle, design of the differential and stability enhancements are to some extent decoupled from the overall torque delivery but, with an independent wheel drive, everything must be co-designed.^{13, 14} In addition, some possibilities (such as integrating motors within the wheel hubs themselves) can add to the unsprung mass of a vehicle, which can cause problems with the vehicle-handling dynamics and vibrations if not correctly dealt with.¹³

It is clear that electric vehicles have an advantage over traditional ICE vehicles in that the designer has considerably more choice in terms of the powertrain architecture.¹⁰ Whereas a conventional vehicle must almost always be a single-drive configuration, a BEV can have a single-drive motor, two independent-drive motors with reducing gears, two independent motors with direct drive or even in-wheel drive.^{9, 10} There is more opportunity for optimising an architecture for a particular usage pattern. At the present time, the key weakness of the BEV is its limited range.⁶ This could in time be solved, and efforts are currently under way in order to increase the battery energy density,¹⁵ to improve the charging infrastructure¹⁶ and to reduce the energy consumption of the vehicle. To obtain the most from a BEV, it is important that the powertrain layout and the sizing are achieved in a way that is at least near-optimal in terms of minimising the energy consumption, and there are established techniques for selecting appropriate vehicle parameters using suitable optimisation techniques.¹⁷

There are several approaches to model-based powertrain optimisation, and an excellent overview can be found in textbook by Guzzella and Sciarretta³ on the subject. Broadly, a researcher must make two choices.

1. A decision must be made on the overall approach to modelling.
2. A decision must be made on the overall approach to optimisation.

There are two broad approaches to modelling; the most conventional is often described as 'forward-facing' modelling. This is perhaps the most natural approach

for engineers, taken by default. In forward-facing modelling, the inputs are the forces and the torques; the outputs are the resulting motions.

In powertrain optimisation, it is common to use models to predict the energy and the fuel requirements associated with particular driving cycles. In these cases, the effective inputs are not the forces but the motions. A forward-facing model can be made to follow a driving cycle, but it is necessary to use some kind of feedback; a driver model is essential. This approach can be very effective but, as with all simulation problems involving feedback, it is slow in execution. Forward-facing models can be made arbitrarily complex and are very good for relatively slow modelling exercises (such as hardware-in-the-loop testing or calibration), but they are more difficult to use for exercises in optimisation where it is necessary either to run a model many times or to perform analytical mathematics on the model. In such cases, it can be preferable to use an alternative ‘backward-facing’ modelling approach, based on quasi-static component models.

Backward-facing models use the motions as their inputs, with the outputs being the forces and the torques required to produce such motions. Generally, fast-acting dynamics are difficult to model and are usually approximated with quasi-static models (see section 4.1.2 of the textbook by Guzzella and Sciarretta³). Models of this kind generally offer less fidelity than their forward-facing equivalents do but, as they do not require driver models or feedback, they are fast in execution. Backward-facing models are used extensively in the literature (see, for example, the papers by Hu et al.¹⁸ and Othaganont et al.¹⁹), and there are also approaches that combine backward-facing models and forward-facing models, using backward-facing models for coarse tuning and forward-facing models for fine tuning.^{20, 21}

Having determined the approach to modelling, it is the necessary to determine an approach for optimisation. Some studies (see, for example, those by Hu et al.¹⁸ and Yang et al.²²) attempted to derive an analytical approximation for their objective functions and then to solve these approximations. This can be used to optimise both the component sizing and the power-split strategy. This has the advantage of computational speed, although it is not always easy to derive the mathematics. For more complex problems, approaches based on parameter search methods are used. Popular algorithmic choices here are genetic algorithms (GA), as used by Hu et al.¹⁸ and Mohan et al.²³

The particular problem which this paper addresses is that at present, although there are techniques for optimising a particular vehicle configuration or even for comparing two or more configurations, there is at present no complete solution to the choice of the most appropriate BEV architecture for the three key objectives: the energy efficiency, the performance (the acceleration) and the affordability. This paper uses multi-objective optimisation to investigate the trade-

offs between these targets for a chosen usage scenario. The approach taken is to evaluate the trade-offs between pairs of objectives, ensuring that the best possible powertrain configurations are chosen through the use of optimisation. This results in a set of guidelines showing how the conflicting objectives interact and indicating the best topology to choose in order to meet any single objective or any pair.

This paper starts by presenting the different BEV topologies considered. Next, it describes the way in which the vehicle and the components were modelled and the multi-objective optimisation used. Then, it shows the results obtained and gives guidelines on topology selection.

BEV powertrain topologies

There are many possible electric vehicle topologies. These are briefly discussed, and a subset is considered for more detailed analysis. The rationale for choosing this subset is also described in detail later. The topologies selected are the single-motor single-axle (SM-SA) topology, the double-motor double-axle (DM-DA) topology, the in-wheel-motor single-axle (IWM-SA) topology and the in-wheel-motor double-axle (IWM-DA) topology and are illustrated in Figure 1.

Single electric machine

There are two possible technologies for a single-machine vehicle: a traditional powertrain formed by adapting a conventional ICE layout, or a specialised design combining the single electric machine with a final-drive gearbox.

Traditional electric vehicle obtained by converting an ICE vehicle. The earliest BEVs were converted from ICE vehicles.²⁴ The ICE and the fuel tank were replaced by an electric machine and a battery pack. To transfer mechanical power from the machine to the wheels, ICE-type transmission components were retained, including a mechanical clutch, a multi-ratio gearbox and a differential. The gearbox can be manual or automatic.¹⁴ Some of the functions of this transmission are unnecessary with an electric vehicle, e.g. the use of the clutch between the motor and transmission, and the use of a complex multi-speed gearbox for matching the torque–speed characteristics of the power plant to the speed and the torque required by the vehicle. (The clutch is entirely unnecessary, and the torque–speed characteristics of the motor are very different from those of an engine.) With this topology, there is still a need for a differential to balance the traction force and the speed between the left traction wheels and the right traction wheels when travelling along a curved path. This topology was designed to be effective for an ICE and not an electric machine; as an electric vehicle, it has a poor efficiency and an excess mass.²⁵

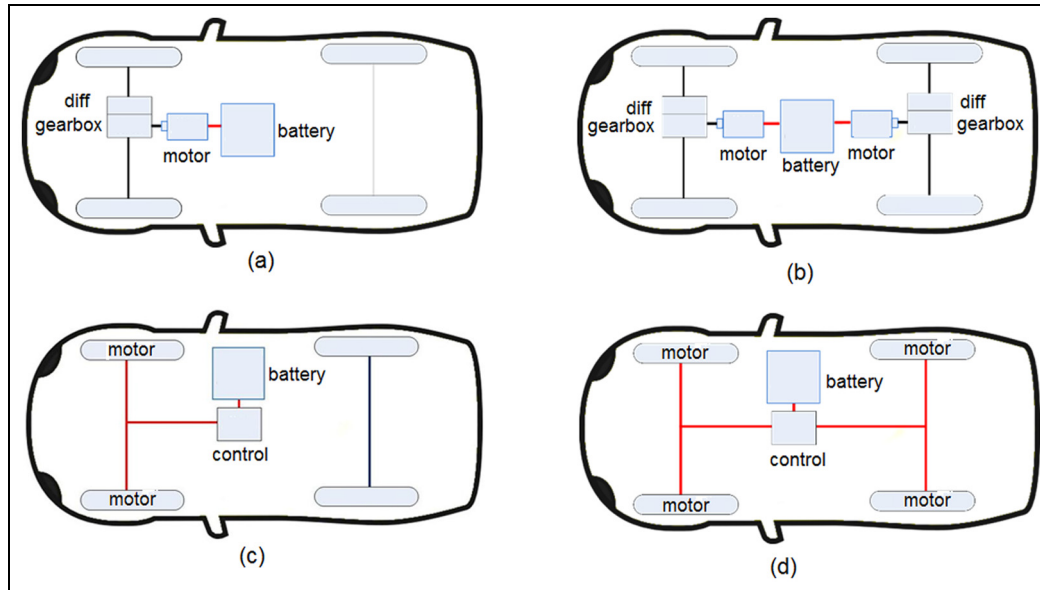


Figure 1. BEV powertrain topologies considered in this study: (a) SB-SA; (b) DM-DA; (c) IWM-SA; (d) IWM-DA. diff: differential.

Single electric machine with a final drive. Electric motors have torque–speed characteristics close to the ideal performance of a vehicle traction power plant and are able to provide near-maximum power in a wide range of speeds. There is a maximum torque at low speeds, because the motor flux is initially constant but, when the machine reaches a base speed, the machine flux weakens whereas the voltage remains constant. As a result, the motor torque decreases as the speed increases; overall, the power remains constant.⁹

With an electric machine, a complex multi-speed transmission is not necessary and, as a result, the complexity of the clutch and gearbox can be eliminated. It is possible to use a light motor, typically a small-sized high-speed low-torque motor, together with a single-speed high-reduction transmission.^{10, 14, 26} For a further reduction in the mass and the inertia, the drive shaft, the motor and the transmission can be integrated as a single component,^{9, 10} as illustrated in Figure 1(a). This type of BEV is predominant in today's marketplace.⁵ However, a central-drive motor with a fixed ratio still encounters mechanical loss. Without a variable gearbox, there is no possibility of operating the motor at its maximum efficiency.²⁷

Multiple-electric-machine drive

Because electric powertrains are relatively simple and because an electric machine can be controlled with good precision, it is possible to use more than one machine at a time, e.g. to have separate motors for each side of a vehicle and/or separate motors for each axle. The following paragraphs describe the topologies used in current research vehicles and prototypes.

Double electric machine with a double-axle drive. Whereas a conventional electric vehicle has a single machine, at either the front axle or the rear axle, each axle can be driven by a separate and independently controlled motor and gearbox. When two traction sources are combined in a single vehicle in this way with an appropriate control strategy, the designer has more degrees of freedom and the flexibility to investigate more effective and efficient operation methods. This powertrain topology is presented in Figure 1(b). This topology has been sufficiently developed for use in a production vehicle, namely the Tesla Model X, introduced in late 2015, which is configured this way, with separate front and rear motors, each with single-ratio gearboxes.²⁸ Vehicles with this topology are operated with a four-wheel drive and are capable of a strong acceleration performance. Tesla, for example, claim that Model X is capable of accelerating from 0 km/s to 100 km/s in less than 5 s, about twice as quickly as a non-performance vehicle.²⁸ This electric vehicle topology still requires the use of a pair of differentials, one front and one rear, which adds mass.

Multiple electric machines with independently driven wheels. It is possible to eliminate the use of differentials by using separate traction motors to drive the wheels on the left and the wheels on the right of a vehicle independently; the speed and the torque of the left wheels and the speed and the torque of the right wheels can be equalised electronically. This tends to improve the overall efficiency by reducing the vehicle mass.²⁹ Without gearing, low-speed high-torque motors are necessary, but fixed gearing, a belt drive or a planetary gearbox can be connected between the motor and the wheels to provide

a better match with commercially available motors. Even with this gearing, eliminating the differential makes more space available, which may be useful for additional battery capacity and a longer range. Moreover, the electronic switching loss can be reduced and the power electronics can be derated.¹⁴ One of the key advantages of this powertrain architecture is an increase in the number of degrees of freedom. With an appropriate energy management strategy, differently specified multiple motors can be configured to spend most of their operating cycle in a more efficient operating envelope than a single motor could achieve, leading to a reduction in the energy consumption.²⁷ The torque balance between the left wheels and the right wheels must be controlled by an electronic differential, which may require complex non-linear control and robust design; failure to operate correctly causes a serious problem for vehicle stability and safety.¹⁴ Furthermore, the cost of two small motors and the associated control units and power electronics is greater than the cost of a single, equivalently powered motor and its associated hardware, adding to the overall cost of the system.^{14, 25}

In-wheel motor drive. Having considered motors closely associated with each wheel, it is natural to wonder whether further benefits can be achieved by integrating the motor into the wheel itself. In-wheel motors for BEVs are the subject of current research,¹¹ however, few passenger cars use in-wheel motors, and most of those that do are still at the research and development stage. In-wheel motor wheels already have applications in mobile robotics.^{27, 30} These applications demonstrate the benefits of in-wheel motors to achieve a high mobility. However, such applications involve only low speeds and focus on the motion of the vehicle rather than on the energy consumption.

In terms of the energy efficiency, the in-wheel motor is integrated into the vehicle wheel which then eliminates all the mechanical gears and the losses associated with transmission.²⁵ The in-wheel motor can therefore make a vehicle lighter. All power is transferred by wire which gives further benefits in terms of the space saving and the flexibility of the component arrangement and also lowers the centre of gravity.^{26, 31, 32} In published literature³³ demonstrating the use of a wheel motor on a motorcycle, it has been shown that, with a wheel motor and using regenerative braking, the overall efficiency can be increased by 20%.

For a passenger car application, there are some disadvantages in terms of the vehicle performance. As with a vehicle with independently driven non-integrated motors, the in-wheel motor requires an electronic differential to follow a curved path; this necessitates a complex torque and speed control between the two sides of the vehicle. Moreover, an integrated in-wheel motor increases the wheel mass and the inertia, adding to the unsprung mass with negative effects on the stability, the safety and the comfort.^{13, 14, 31, 34}

In contrast, there are some positive vehicle dynamics aspects of using in-wheel motors. It has been shown that using in-wheel motors with a direct drive can have advantages in terms of the vehicle stability and control, because the in-wheel motors have a quick torque response and allow easy torque measurements.³⁵ This makes it easier to implement integrated vehicle dynamic control and features such as an anti-lock braking system and dynamic tracking control compared with those in conventional ICE vehicles.^{14, 35, 36, 37} In-wheel drives have been used in a four-wheel-drive electric vehicle to implement an electrically torque-assisted steering system and global torque control for a four-wheel independent-drive electric vehicle.³⁸ Because they do not use gearing, in-wheel motors need to be able to produce a high torque at a low speed, which may result in greater losses compared with those of a traditional electric motor owing to the required higher currents. There are efforts to design appropriate machines for this application, such as the axial-flux permanent-magnet machine, and this helps in the design and selection of suitable in-wheel motors for use in BEVs.^{14, 26, 31}

Selected BEV powertrain topologies

The previous section presented several architectures with their associated permutations. A subset of these must be chosen for detailed analysis using multi-objective optimisation, including a cost–benefit analysis. The literature contains techniques for identifying parameter sets producing the greatest sensitivity in terms of the energy consumption,²⁰ highlighting the importance of the powertrain efficiency and suggesting that the benefits of multi-ratio transmissions are likely to be marginal. Consequently, variable-ratio gearing systems were not considered in this work. Four powertrain topologies were selected for detailed analysis, all using a single-ratio transmission where appropriate (the in-wheel drive version is naturally gearless and so the ratio is unity). These topologies are illustrated above in Figure 1 and are the SM-SA topology (the Nissan LEAF can be taken as a benchmark), the DM-DA topology, the IWM-SA topology and the IWM-DA topology. The significant differences in terms of modelling are explained next.

Vehicle model and simulation technique

Vehicle modelling techniques can be classified in two ways: forward-facing models and backward-facing models. The literature discusses the advantages and disadvantages of these two simulation methods,^{18, 21} and a brief description is provided in the following sections.

Forward-facing simulations

Forward-facing simulations present a realistic approach to vehicle simulations as they use a driver model to control the vehicle speed, similar to a human driver

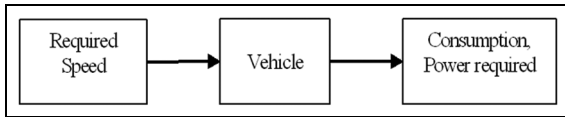


Figure 2. Backward-facing model of the vehicle showing the trajectory as the input.

controlling a car. Figure 2 illustrates the structure of generic forward-facing simulations. Starting from the driver model, the reference speed and the actual vehicle speed are compared, giving an ‘error’ signal, and this is used to generate a control signal to control the torque used to power the vehicle. (Driver models normally use proportional–integral controllers). In practice, the source of power of the BEV is an electric motor, and so an appropriate model is used to translate the throttle and brake commands from the driver into the torque and mechanical braking signals. The torque from the motor is passed through a model of the transmission and applied as a force at the wheels. The longitudinal dynamics of the vehicle are then modelled; it is usually assumed that we can consider the vehicle as a whole, ignoring the separate inertias associated with the wheels and the machines. Lateral dynamics are ignored.

The advantage of forward-facing simulations is that they are realistic because of higher fidelity. This method is used for designing the vehicle hardware and detailed control development. However, this has to be traded off against the computation overheads; simulations are expensive and time consuming.

Backward-facing simulations

Backward-facing simulations use the opposite approach. In forward-facing models, the inputs of the components are the generalised forces and the outputs are the generalised motions whereas, in backward-facing models, the inputs are the generalised motions and the outputs are the generalised forces. Consequently, the speed references can drive the system model directly, and a driver model is not required. One assumption made with backward-facing simulations is that the vehicle exactly follows the driving cycle, as illustrated in Figure 3. In the diagram, the driving profile is the speed that the vehicle is required to follow. The traction-resultant forces of the vehicle are calculated from the vehicle model. The principle of conservation of power is applied from one component to the next. The resultant forces and speeds at the contact patch between the tyres and the road are converted from the torque and the angular velocity to the torque and the speed required at the gearbox. The power required from the gearbox, including the gearbox losses, is then transferred to the electric motor model and the battery model.

Backward-facing simulations generally rely on quasi-static component maps rather than on detailed dynamic

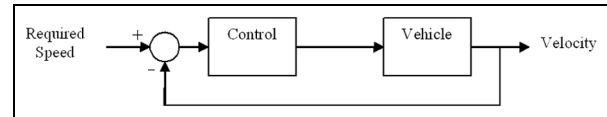


Figure 3. Forward-facing model of the vehicle showing the driver feedback loop.

models. Electric machines are typically modelled using motor efficiency maps. These are lookup tables indicating the efficiency achieved for any required torque–speed pair. The data for this can be collected from the testing of a real electric machine in steady-state conditions. This simulation type cannot represent the dynamic behaviour of components because it is not usually possible to invert the dynamics exactly; this is a disadvantage in comparison with forward-facing simulations. However, for energy efficiency calculations and optimisation, backward-facing simulations require less time and fewer computational steps than those required for forward-facing simulations.

Vehicle body and environmental losses

The vehicle model converts the velocity reference into the angular velocity and the torque at the wheels, as presented in Figure 4. The angular velocity at the wheels can be calculated from

$$\omega_w(t) = \frac{v_{vehicle}(t)}{r_w} \quad (1)$$

where ω_w is the angular velocity at the wheel, $v_{vehicle}$ is the velocity of the vehicle and r_w is the radius of the wheel. The torque at the wheels is given by

$$T_w(t) = F_{vehicle}(t)r_w \quad (2)$$

where T_w is the torque at the wheel and $F_{vehicle}$ is the traction force at the centre of gravity. $F_{vehicle}$ is calculated from the environmental force that applies to the vehicle according to

$$F_{vehicle}(t) = MgC_r + \frac{1}{2}\rho C_d A v_{vehicle}^2(t) + M \frac{dv_{vehicle}(t)}{dt} \quad (3)$$

where M is the vehicle mass, g is the acceleration due to gravity, C_r is the rolling resistance of the vehicle, ρ is the density of air and C_d is the drag coefficient. Losses from the environmental force result from the aerodynamic resistances, the rolling resistances of the tyres and the vehicle climbing the slope. However, these simulations are applied only when the vehicle is moving on a flat road; accordingly, the loss from hill climbing is neglected.

Transmission

Like ICEs, electric machines operate most efficiently within a particular speed–torque envelope. With the

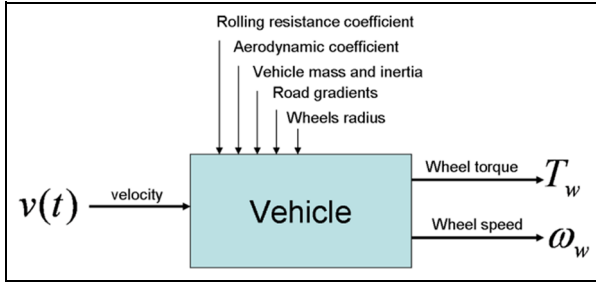


Figure 4. Inputs and outputs of backward-facing simulations of the vehicle.

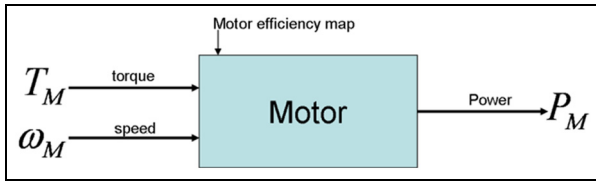


Figure 5. Inputs and outputs of backward-facing simulations of the motor-machine.

notable exception of wheel motors, most of the machines used in electric vehicles operate best at higher speeds and lower torques than those encountered at the driveshaft; the transmission transforms the speed-torque pair at the machine to a different speed-torque pair at the driveshaft with equal power. The transmission normally includes several components but, in this work, we consider those using a single ‘lumped’ gear ratio which describes the overall behaviour. As discussed earlier, there is no need for multiple ratios, and single-ratio transmissions are common on production vehicles.^{7, 28} Single-speed transmissions are generally good in terms of a low drivetrain mass, a low volume, a high efficiency and a low complexity.^{9, 39}

The calculations for the transmission are expressed as

$$\omega_M(t) = \omega_w(t) \times \text{gear ratio} \quad (4)$$

$$T_M(t) = \frac{T_w(t)}{\text{gear ratio} \times \eta_G} \quad (5)$$

where ω_M is the angular velocity at the motor, ω_w is the angular velocity at the wheels, T_M is the torque at the motor, T_w is the torque at the wheels and η_G is the efficiency of the transmission.

Electric machine modelling

The electric machine acts as a motor-generator, providing a traction torque during acceleration and steady-state driving and then recovering the kinetic energy that is otherwise lost during braking. A schematic diagram for a backward-facing model is shown in Figure 5. The relationship between the motor input power and the output torque-speed pair is given later in equation (6).

Note that the machine is not perfectly efficient. When motoring, the machine output power is given by $\eta_M P_M$, where P_M is the power (kW) and η_M is the efficiency (dimensionless) of the motor. When the equation is arranged as a backward-facing model, the efficiency term appears as a division rather than a multiplication. The efficiency term $\eta_M < 1$ when motoring. (When generating, the equation can be kept the same but the efficiency term needs to be set so that $\eta_M > 1$.) Note that this is a mathematical construct; the system is still ‘lossy’ in both directions.

The use of a motor map for the backward-facing simulations has been described and, for quasi-static vehicle simulations, it is possible to calculate the energy consumption of the electric machine by using a static map, as presented by Lukic and Emado.⁴⁰ The efficiency is calculated as a function of the torque, the speed and the motor parameters. (This is described in greater depth in the next section.) The relevant formulae are

$$P_M(t) = \frac{T_M(t)\omega_M(t)}{\eta_M} \quad (6)$$

and

$$\eta_M = f(T_M, \omega_M, \phi_M) \quad (7)$$

where ϕ_M is the motor rating (kW).

Electric machine modelling with efficiency maps

A motor efficiency map is a two-dimensional lookup table that contains information on the motor efficiency. The motor efficiency is a function of the motor torque and the speed as described in equation (7). This motor map describes the steady-state efficiency, and this information is usually collected by measuring the power when motors are tested with a dynamometer. To model machines of different sizes, techniques adapted from the literature were used; in the textbook by Guzzella and Sciarretta,³ the machine efficiency map is made scalable to provide a representation of different-sized machines. The toolbox used by Guzzella and Sciarretta contains a lookup table of the electric machine efficiency in both the motor mode and the generator mode. A similar approach was taken in this work. The starting point was the nominal machine map for the machine of the case-study vehicle. To scale it, the torque axis was scaled in proportion to the machine’s power rating; this principle is illustrated in Figure 6.

Figure 7 shows the plot of the motor efficiency map which is converted from the original 80 kW motor of the Nissan LEAF.⁴¹ This map was used for the optimisation process; this modification assumes that the speed of the motor is limited to 10,500 r/min for every size of motor. A peak torque and efficiency map was constructed for a standard size of the Nissan LEAF motor. The original motor power (80 kW) and peak torque (280 N m) are used for the base map. The torque axis is

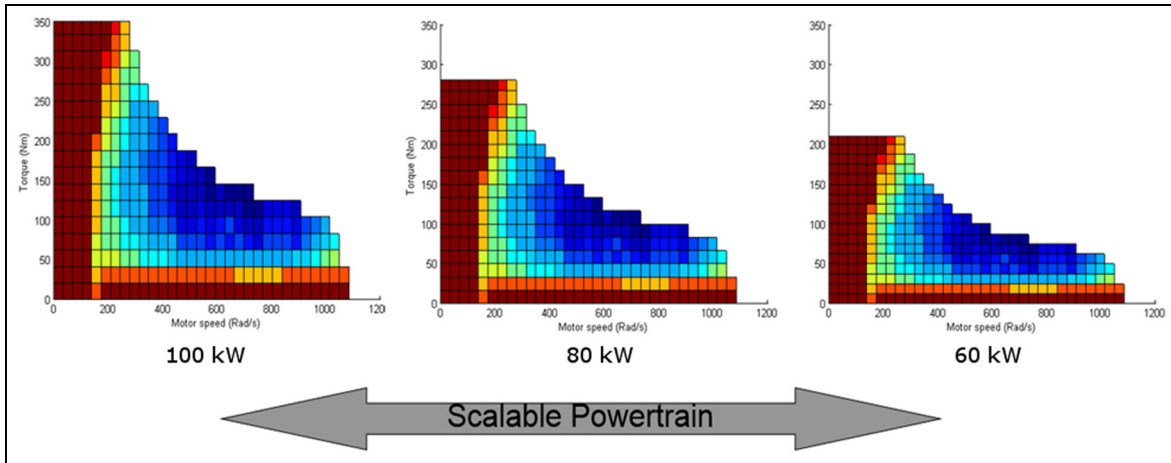


Figure 6. Scalable motor map for the permanent-magnet synchronous motor.

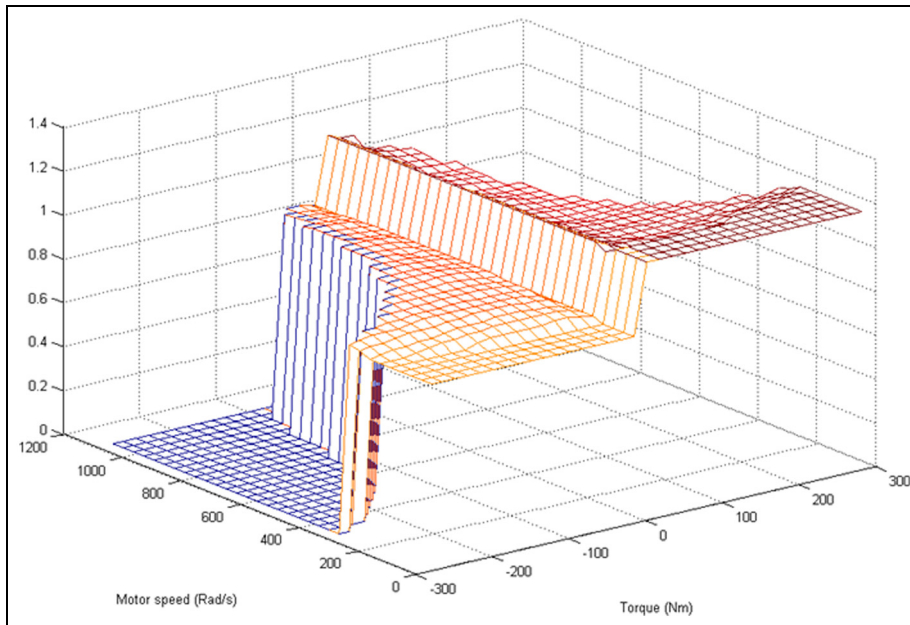


Figure 7. Motor efficiency map (implemented in the model lookup table).

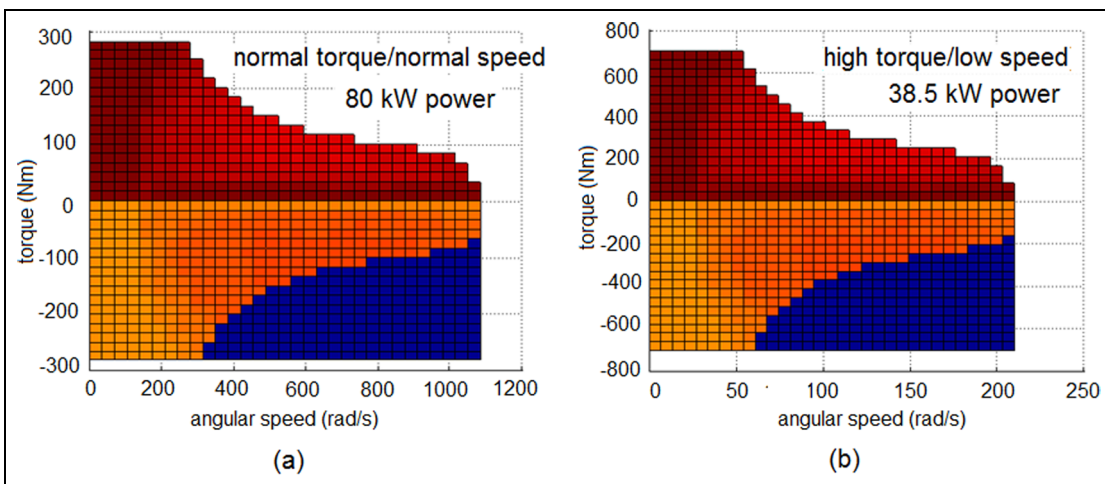


Figure 8. (a) Original motor map for conventional motors; (b) modified motor map assumed for in-wheel vehicles.

then scaled to represent differently sized motors. For example, for a 60 kW motor, a scale factor of 0.75 is used. A similar technique is used for both traction and regenerative braking, where a positive torque represents the motor efficiency in the traction mode and a negative torque represents the regenerative braking efficiency.

Significant factors which affect the efficiency of electric motors include the size, the mass and the method of motor cooling. Different powertrain architectures use different numbers of motors and different motor sizes. For the same power requirement, a centre drive needs a single high-powered electric motor. On the other hand, an independent drive considers two or four small motors, the total power of which is equal to that requirement. As a result, the size, the mass and the method of motor cooling may influence the powertrain design. In general, a larger motor is likely to be more efficient than a smaller motor is. When increasing the motor power, an increase in the motor speed results in a better motor efficiency than an increase in the motor torque does. This is because the losses in the motor are directly proportional to the motor current, which is related to the torque rather than the power. Hence, at the same power, a low-speed high-torque motor is more likely to have higher losses. In terms of the motor size, a high-speed motor with a gearbox is smaller than a low-speed high-torque motor alone.²⁵

Modified motor map for in-wheel motors

In the first two cases (SM-SA and DM-DA vehicles), a scalable motor map of the permanent-magnet synchronous machine motor is used, as presented in Figure 8. However, for in-wheel motor vehicles (IWM-SA and IWM-DA vehicles), the torque–speed characteristics are different, as in-wheel motors require a high torque at a low speed. For a reasonable comparison between a conventional motor and an in-wheel motor, the in-wheel motor efficiency map is based on the original map of the Nissan LEAF. The torque scale and the speed scale were modified to match the in-wheel motors available on the market.^{42, 43} Specifications from a manufacturer of in-wheel motors shows a peak torque of around 700 N m and a maximum speed of around 2000 r/min; the original motor map provides a peak torque at 280 N m, based on a speed of 280 rad/s and a maximum speed of 1100 rad/s, and delivers a power of up to 80 kW. For the in-wheel motor, the torque scale is extended by a factor of 2.5 at the torque axis to obtain a maximum torque of up to 700 N m and is based on a speed of 53 rad/s and a maximum speed of 210 rad/s. The peak power becomes 38.5 kW, as presented in Figure 8. The scaling was chosen so that the in-wheel motor map represents half the power of the original map because the in-wheel vehicle requires at least two identical motors to drive each wheel (for a single-axis drive), and each motor needs to provide only half the overall power.

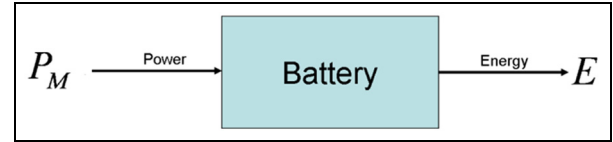


Figure 9. Input and output of backward-facing simulations of the battery.

Battery

The battery is the main source of energy for the BEV. It is an electrochemical device that stores electrical energy in the form of chemical energy. In this research, a simple battery model is used. A static model of this battery model consists of an open-circuit voltage source and an internal resistance. A schematic diagram is presented in Figure 9.

State of charge. The state of charge (SOC) of the battery is the amount of charge $Q(t)$ that remains in the battery relative to the capacity Q_{bat} (A h) of the battery, as given by

$$\text{SOC} = \frac{Q(t)}{Q_{bat}} \quad (8)$$

with

$$Q(t) = Q_{init} - \int I_{T,bat}(t) dt \quad (9)$$

where Q_{init} is the initial charge of the battery and $I_{T,bat}(t)$ is the terminal current of the battery, where a positive current discharges the battery and a negative current charges the battery. The current at the terminal of the battery can be calculated as a function of the power that is required from the battery and the terminal voltage of the battery, as described by

$$I_{T,bat}(t) = \frac{P_M}{V_{T,bat}} \quad (10)$$

with

$$V_{T,bat} = V_{OCV,bat} - I_{T,bat}(t)R_{i,bat} \quad (11)$$

The terminal voltage $V_{t,bat}$ is calculated from the open-circuit voltage $V_{OCV,bat}$, as shown in Figure 10, and the internal resistance $R_{i,bat}$ of the battery from

$$V_{T,bat}^2 - V_{OCV,bat}V_{T,bat} + P_MR_{i,bat} = 0 \quad (12)$$

By substituting current $I_{T,bat}(t)$ from equation (10) into equation (11), the terminal voltage can be calculated as a function of the power, the open-circuit voltage and the internal resistance according to

$$V_{T,bat} = \frac{V_{OCV,bat} + \sqrt{V_{OCV,bat}^2 - 4P_MR_{i,bat}}}{2} \quad (13)$$

Pack-level calculations. The terminal voltage of the battery and the capacity of the battery are calculated from the series–parallel combinations of battery cells, as shown

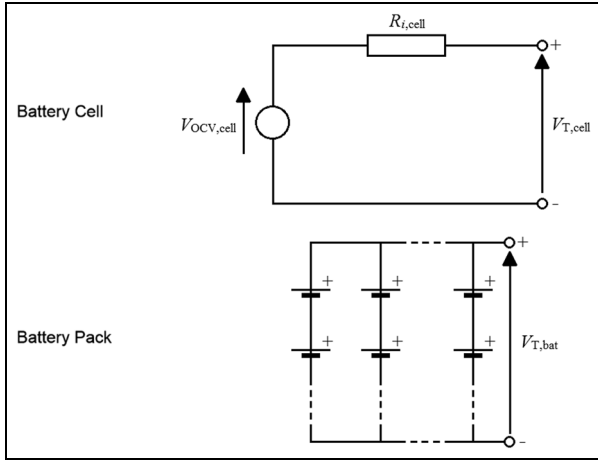


Figure 10. Cell model and battery pack model for the electric vehicle.

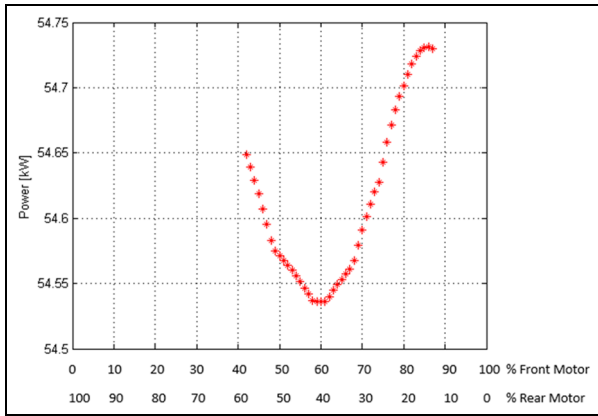


Figure 11. Relationship of the power requirement to the torque split.

in Figure 10. The open-circuit voltage of a battery pack is calculated from the open-circuit voltage of a cell and the number of cells in series, as given by

$$V_{OCV,bat} = V_{OCV,cell} N_{series} \quad (14)$$

The battery capacity can be calculated from

$$\text{Battery capacity (kW h)} = N_{series} N_{parallel} \times \text{cell capacity (kW h)} \quad (15)$$

where N_{series} is the number of cells in series and $N_{parallel}$ is the number of cells in parallel.

Motor torque-split control

To drive simultaneously a vehicle with more than one axle, e.g. a four-wheel-drive vehicle, there is a need for a device to split the torque between the axles. For the conventional vehicle (ICE), this is achieved with a central differential. For the BEV, a torque split can also be used to maximise the energy efficiency; for any given

power demand, there is an optimally efficient way of splitting the torque between the front machine and the rear machine. When a quasi-static model is assumed, this optimal split can be achieved with a deterministic algorithm, which selects the most efficient operating point for each motor using the torque–speed curves and the efficiency maps. The front motor and the rear motor can be the same size or different sizes, and the effects of transmission can be taken into account; it is possible to use different ratios for the front and the rear. Calculation is easy and does not require online optimisation; in the model, the torque-split function was implemented using a lookup table to create a split ratio as presented in the following.

The total motor output is given by

$$P_{out,total} = T_F \omega_{M,front} + T_R \omega_{M,rear} \quad (16)$$

where T_F is the torque of the front machine, $\omega_{M,front}$ is the speed of the front machine, T_R is the torque of the rear machine and $\omega_{M,rear}$ is the speed of the rear machine. These can be related to the wheel speeds via the front gear ratio G_F and the rear gear ratio G_R by

$$P_{out,total} = T_F \frac{\omega_w}{G_F} + T_R \frac{\omega_w}{G_R} \quad (17)$$

T_F can be expressed as a fraction T_S of the required torque that it needs to supply if only the front motor was used, according to

$$T_F = T_S \frac{P_{out,total}}{\omega_w / G_F} \quad (18)$$

This then requires the equivalent relationship for the rear motor given by

$$T_R = (1 - T_S) \frac{P_{out,total}}{\omega_w / G_R} \quad (19)$$

If the machine efficiencies $\eta_F(T_F, \omega_F)$ and $\eta_R(T_R, \omega_R)$ are functions of the torque and the speed, the problem becomes how to minimise the instantaneous power, which is given by

$$P_{in,total} = \frac{T_F \omega_{M,front}}{\eta_F(T_F, \omega_F)} + \frac{T_R \omega_{M,rear}}{\eta_R(T_R, \omega_R)}$$

Minimisation is achieved by

$$T_S = \arg \min \left(\frac{T_S P_{out,total}}{\eta_F\{T_S [P_{out,total} / (\omega_w / G_F)], \omega_w / G_F\}} + \frac{(1 - T_S) P_{out,total}}{\eta_R\{(1 - T_S) [P_{out,total} / (\omega_w / G_R)], \omega_w / G_R\}} \right) \quad (20)$$

This is a static relationship for any given output-power–wheel-speed pair and can be precomputed as a lookup table for convenient implementation.

Figure 11 presents the operating points of the 48 kW front motor and the 32 kW rear motor. A total torque of 100 N m is required from the two motors. The torque-split function selects the operating point as

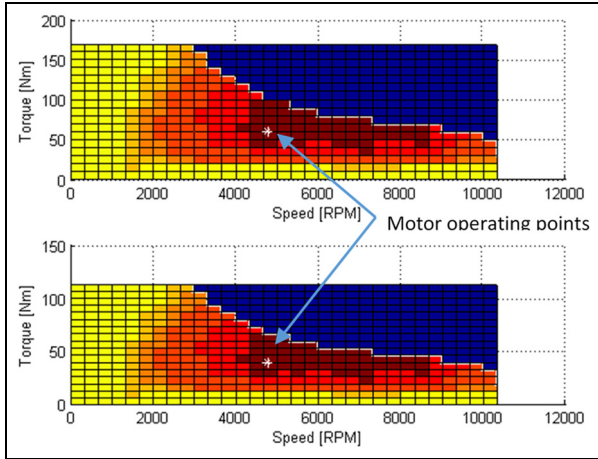


Figure 12. Power consumptions for two motors with torque splitting.
RPM: r/min.

follows: a torque of 60 N m from the front motor and a torque of 40 N m from the rear motor. With the 60%-front-split ratio, both motors operated with minimum energy consumptions, as presented in Figure 12.

The torque-splitting algorithm is used in the traction mode only; the torque split in regenerative braking remains constant, depending on the size of the motors, as expressed by

$$T_{SB} = \frac{\phi_F}{\phi_F + \phi_R} \quad (21)$$

where T_{SB} is torque split in the braking mode, ϕ_F is the front-motor rating (kW) and ϕ_R is the rear-motor rating (kW). This ensures that the braking force from the front wheels is always greater than or equal to the braking force from the rear wheels. During braking, this approach cannot be used; the stability of the vehicle can potentially become an issue, and so there are strict legislative requirements governing the proportion of the braking force that can be applied at each axle. The torque-splitting algorithm is employed when the vehicle is accelerating or maintaining a constant speed.

Mass of the vehicle

In this section, we investigate the effect of different vehicle topologies, as discussed before, on the energy consumption and the acceleration performance. One of the important vehicle parameters which impacts the energy consumption is the mass of the vehicle.²⁰ The mass of the vehicle is calculated by considering three components: the electric machine and the transmission (combined), the battery and the vehicle body.

Mass of the transmission and the electric machine. For mass calculations, the electric machine and its transmission are treated as a single unit. For the SM-SA and DM-DA vehicles, each axle is equipped with a single-ratio

transmission only, and it is assumed that the difference between the masses of gearboxes with different transmission ratios is negligible. The mass of the motor is estimated by using the average mass of the permanent-magnet motors available commercially.⁴⁴ Table 1 gives the formulae used.

Table 2 details assumptions made on the mass of the transmission components. In the DM-DA type, the mass of the additional transmission which is 30 kg, is added to the total vehicle mass; a 25% mass reduction was applied to the overall powertrain mass for in-wheel vehicles as they do not have a transmission and a drive shaft.

From these tables it can be seen that, if the vehicle has a fixed electric machine power (80 kW for the SM-SA vehicle and 40 kW + 40 kW for the DM-DA vehicle), the DM-DA type is always heavier than the SM-SA type. This is not surprising and, if there are no other changes to the vehicle, a DM-DA powertrain needs to be operated more efficiently to provide an advantage in terms of the energy consumption relative to the SM-SA powertrain.

Mass of the battery. The mass of the battery pack was estimated from the number of cells in the battery. The cells and the pack size used in the Nissan LEAF⁴⁵ were used as the baseline. Each cell has a mass of 0.787 kg, and there are four cells in one module and 48 modules in a battery pack, giving a total cell mass of $0.787 \times 4 \times 48 = 151.1$ kg. It is assumed that a battery also requires 0.06 kg/kW for the mass of the thermal management system and 0.14 kg/kW for the mass of the harness and the bus bar; this gives an effective total cell mass of 0.975 kg per cell. Using these assumptions, the total mass of the case-study Nissan LEAF was estimated to be 187.2 kg. In this work, the mass of the battery in every topology is calculated using the same formula, since a similar type of battery pack is assumed, although the number of cells is allowed to vary.

Calculation of the kerb mass of the vehicle. For these calculations, it is assumed that the vehicle is of a similar type to the original-case-study vehicle, namely a C-segment passenger car. The mass of a vehicle can be considered to consist of the mass of the powertrain plus a ‘glider’ mass, i.e. the fixed mass of the vehicle without the powertrain components. (This terminology comes from the aerospace domain; an aircraft without an engine is a glider in a literal sense!) The total mass M_{orig} of the case-study vehicle is 1521 kg. To estimate the glider mass M_{glider} , the mass M_{PTorig} of the powertrain of the case-study vehicle was estimated using the formulae already presented; this was subtracted from the total mass to obtain an estimate of the glider mass as

$$M_{glider} = M_{orig} - M_{PTorig} \quad (22)$$

This calculation described assumes that the glider mass is unaffected by the choice of powertrain. In practice,

Table 1. Assumed motor masses for each topology.

Topology	Assumed mass (kg) of the following	
	Front electric machine	Rear electric machine
SM-SA	$0.532P_{motor,kW} + 21.6$	No motor
DM-DA	$0.532P_{motor,kW} + 21.6$	$0.532P_{motor,kW} + 21.6$
IWM-SA	$(0.532P_{motor,kW} + 21.6) \times 2$	No motor
IWM-DA	$(0.532P_{motor,kW} + 21.6) \times 2$	$(0.532P_{motor,kW} + 21.6) \times 2$

SM-SA: single-motor single-axle; DM-DA: double-motor double-axle; IWM-SA: in-wheel-motor single-axle; IWM-DA: in-wheel-motor double-axle.

Table 2. Assumed transmission masses for each topology.

Topology	Assumptions made regarding the powertrain component mass
SM-SA	Default, unchanged from the case-study vehicle
DM-DA	Front axle as SM-SA, additional 30 kg added for the rear axle
IWM-SA	Reduction of 25% compared with SM-SA
IWM-DA	Reduction of 25% compared with SM-SA

SM-SA: single-motor single-axle; DM-DA: double-motor double-axle; IWM-SA: in-wheel-motor single-axle; IWM-DA: in-wheel-motor double-axle.

Table 3. Assumed costs of the powertrain components for each topology.

Topology	Assumed cost (US\$) of the motors and the transmission		
	Front motor(s)	Rear motor(s)	Transmission
SM-SA	$16P_{motor,kW} + 385$	No motor	As case study
DM-DA	$16P_{motor,kW} + 385$	$16P_{motor,kW} + 385$	Second gearbox + 5%
IWM-SA	$(16P_{motor,kW} + 385) \times 2$	No motor	As case study
IWM-DA	$(16P_{motor,kW} + 385) \times 2$	$(16P_{motor,kW} + 385) \times 2$	As case study

SM-SA: single-motor single-axle; DM-DA: double-motor double-axle; IWM-SA: in-wheel-motor single-axle; IWM-DA: in-wheel-motor double-axle.

this is unlikely to be true; a heavier powertrain probably requires a stronger and heavier chassis, for example. To model this, it was assumed that the chassis would be made heavier by 0.6 times the increase in powertrain mass according to

$$M_{new} = M_{glider} + M_{PTnew} + 0.6(M_{PTnew} - M_{PTorig})$$

or, more simply,

$$M_{new} = M_{orig} + 1.6(M_{PTnew} - M_{PTorig}) \quad (23)$$

Calculation of the powertrain cost

Table 3 gives the equations and the assumptions made for calculating the cost of the powertrain. These equations are based on the long-term pricing estimates from the literature.⁴⁴

The pack cost is based on the capacity of the pack and the cell cost, which is itself dependent on the power-to-energy ratio P/E of the cells; P/E was taken to be 4.0 based on the information available for the Nissan LEAF.⁴⁵ The formulae for the costs are

$$\text{Cell cost(US\$/kW h)} = 11.1 \times \frac{P}{E} + 221.1 \quad (24)$$

$$\text{Cost}_{battery\ pack}(\text{US\$}) = [\text{cell cost(US\$/kW h)} + 13] \times \text{cell capacity (kW h)} + 680 \quad (25)$$

The total mass and cost of the powertrain are calculated on the basis of the the mass and cost of the motor according to

$$\text{Cost}_{powertrain} = \text{cost}_{motor} + \text{cost}_{powertrain} + \text{cost}_{battery\ pack} \quad (26)$$

Details of these calculations can be found in Table 3.

Calculation of the driveability (the acceleration time)

The driveability is assessed using a simple calculation to estimate the time taken to accelerate from rest to 100 km/h.

It is assumed that the quasi-static representation of the system is correct. Given a vehicle of constant mass M , let $v(t)$ be the instantaneous speed of the vehicle, and let $f_w(v)$ be the maximum tractive force at that speed. Consider Newton's second law applied over a small time window according to

$$f_w(v) = \frac{M(v + \delta v) - Mv}{\delta t} \quad (27)$$

Table 4. Masses of the powertrain components for each topology prior to any optimisation, assuming a total motor power of 80 kW.

Topology	Front motor	Rear motor	Transmission mass	Difference from the Nissan LEAF (kg)
SM-SA	One motor at 80 kW and 64.16 kg	No motor	As case study	± 0.0
DM-DA	One motor at 40 kW and 42.88 kg	One motor at 40 kW and 42.88 kg	30 kg added (rear gearbox)	+ 51.6
IWM-SA	Two motors each at 40 kW and 42.88 kg	No motor	25% reduction	+ 0.16
IWM-DA	Two motors each at 20 kW and 32.24 kg	Two motors each at 20 kW and 32.24 kg	25% reduction	+ 32.6

SM-SA: single-motor single-axle; DM-DA: double-motor double-axle; IWM-SA: in-wheel-motor single-axle; IWM-DA: in-wheel-motor double-axle.

Table 5. Energy efficiencies for each topology prior to optimisation, assuming a total motor power of 80 kW.

Topology	Vehicle mass (kg)	Acceleration time (s)	Cost (US\$)	Energy consumption (kW h/100 km)
SM-SA	1520	9.9	8900	16.5
DM-DA	1570	10.5	9300	16.6
IWM-SA	1520	11.2	9300	16.0
IWM-DA	1550	11.5	10,100	16.1

SM-SA: single-motor single-axle; DM-DA: double-motor double-axle; IWM-SA: in-wheel-motor single-axle; IWM-DA: in-wheel-motor double-axle.

Rearranging this gives

$$\delta t = \frac{M}{f_w(v)} \delta v \quad (28)$$

Summing both sides over the acceleration period and taking the limit give

$$T = \int_0^T dt \quad (29)$$

$$= \int_0^V \frac{M}{f_w(v)} dv$$

where V is a specified speed and T is the time taken to reach that speed. Thus, the time taken to reach a speed of 100 km/h (27.78 m/s) from rest can be estimated from

$$\begin{aligned} (\text{Acceleration time})_{0-100\text{ km/h}} &= T_{100} \\ &= \int_0^{27.78} \frac{M}{f_w(v)} dv \end{aligned} \quad (30)$$

where T_{100} is the time taken to accelerate from rest to 100 km/h.

Vehicle simulations without optimisation

In order to understand the implications of each chosen topology, two studies were carried out. In the first study, the properties of each topology with an 80 kW electric machine were considered. The battery pack was kept at the case-study size, and there were no attempts to optimise

the powertrain. The aim of this part of the study was to demonstrate that the basic methodology was sensible and that the simulations gave reasonable results.

For the SM-SA topology, a single 80 kW motor at a front axle is used, as in the case-study vehicle. For the DM-DA topology, two identical motors are applied, one at the front and the other at the rear. For the IWM-SA topology, two 40 kW in-wheel motors are used, one each at the left side and the right side of the front axle; for the IWM-DA topology, four 20 kW in-wheel motors are used. Table 4 shows the difference in the powertrain masses; the DM-DA vehicle has the most extra mass because it is using an additional motor and gearbox at the rear axle. For in-wheel topologies, four motors are used, but this is offset by the reduction in the powertrain mass due to the omission of gearing.

Table 5 shows the results of simulations, namely the energy consumptions, the acceleration times and the powertrain costs. It can be seen that both the in-wheel motor vehicles consume less energy than the original-case-study vehicle does. The worst is the DM-DA vehicle although, despite the fact that its mass increases by over 3% or 50 kg owing to the rear-axle motor and transmission, the energy consumption increased by only around 1% in comparison with that of the case-study vehicle; this is because efficiencies arise from the motor torque split which divides the vehicle torque between the front axle and the rear axle efficiently.

Multi-objective optimisation for different BEV topologies

To obtain a fair comparison of the benefits of each topology, it is important to assess them at their best.

This means optimising the whole powertrain, with all significant parameters, e.g. the machine power and the battery sizing, and, where appropriate, the gear ratios. For the DM-DA topology, the front machine and the rear machine were permitted different motor sizings and different gear ratios.

The multi-objective optimisation problem chosen for this assessment considered the simultaneous minimisation of three objectives: first, the real-world energy consumption over the Common Artemis Driving Cycle (CADC); second, the acceleration time from 0 km/h to 100 km/h; third, the powertrain cost. These three objective functions are equally weighted. A constraint on the range was applied; when using the NEDC (currently required for legislative statements in the UK), the range of the vehicle had to be at least 175 km. This ensures that any vehicle produced gives a comparable range with the Nissan LEAF. Optimisation was performed using readily available GA solvers from the MATLAB R2014a Global Optimisation Toolbox's 'ga' command; the user's guide for this software details in some depth the algorithms used.⁴⁶ It is beyond the scope of this paper to describe the details in depth but, to aid the reader, the fundamentals are recapped here. The essential idea of a GA is to mimic Darwinian evolution by natural selection. In place of the usual objective function, GA theorists talk about a scalar-valued fitness function. Any given point in the optimisation space has a fitness function. The idea is to start with a random population of points in the design space, to select the fittest (i.e. those with the best objective function values) and then to cross-breed the selected points to create children with inherited properties which are a mix of those of their parents; to ensure that this is not too limiting, the children may also incorporate mutations, introducing a degree of randomness into the process. Over successive generations, the population tends to become fitter and eventually to converge the fittest possible. As with all attempts at non-convex optimisation (other than the impossible, fully exhaustive search), there is always a risk that the process settles on a sufficiently attractive local minimum rather than the true global minimum, although the fact that the initial points are distributed through the design space and the presence of mutations can help to reduce this risk. A degree of confidence can be obtained from the fact that GAs have been successfully used in powertrain component sizing optimisation, where they have confirmed the near-optimality of the Nissan LEAF.⁴⁷

A mathematical formulation for the problem of this paper is given as follows: minimise

$$J_1(X_D), J_2(X_D), J_3(X_D) \quad (31)$$

where

$$J_1(X_D) = E(X_D) = \text{cycle energy consumption} \quad (32)$$

$$J_2(X_D) = (\text{acceleration time})_{0-100 \text{ km}} \quad (33)$$

$$J_3(X_D) = \text{cost}_{\text{powertrain}} \quad (34)$$

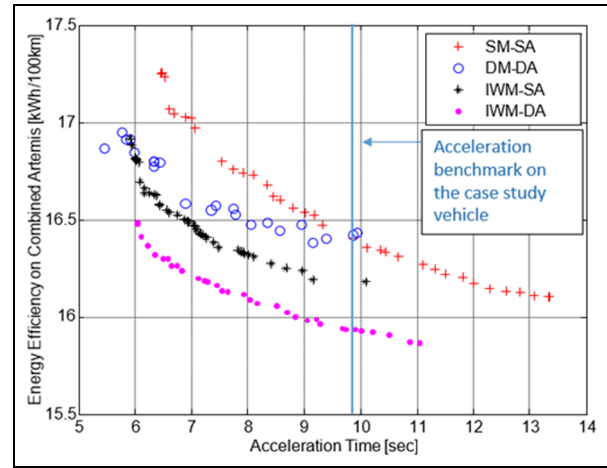


Figure 13. Pareto front of the acceleration time and the energy consumption.

SM-SA: single-motor single-axle; DM-DA: double-motor double-axle; IWM-SA: in-wheel-motor single-axle; IWM-DA: in-wheel-motor double-axle.

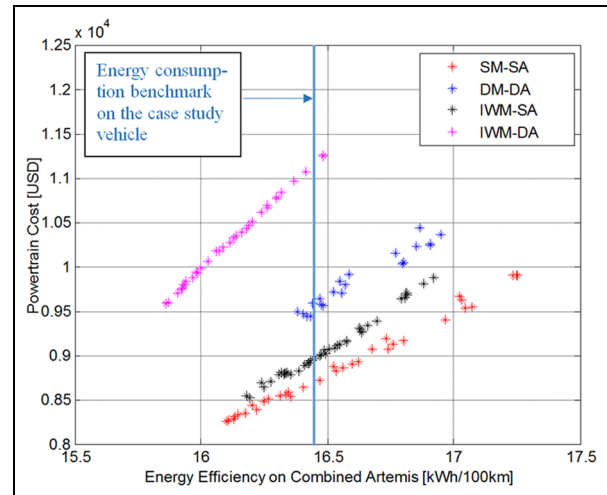


Figure 14. Pareto front of the energy consumption and the powertrain cost.

USD: US\$; SM-SA: single-motor single-axle; DM-DA: double-motor double-axle; IWM-SA: in-wheel-motor single-axle; IWM-DA: in-wheel-motor double-axle.

subject to

$$\text{Range(NEDC)} \geq 175 \text{ km} \quad (35)$$

where X_D is a vector of the vehicle parameters such as motor size, the gear ratio and the battery capacity and T is the time (s) of a driving cycle. The results of the multi-objective optimisation are shown in Figures 13 and 14. Figure 13 shows the trade-offs of between the energy consumption and the acceleration time for each topology. The vertical solid line shows as a benchmark the acceleration of the Nissan LEAF, 9.9 s for 0–100 km/h. For each topology, it is possible to match or improve the original acceleration performance relative to the benchmark vehicle; this is most noticeable for

Table 6. Energy consumption for each topology after optimisation, subject to a constraint of meeting a specified driveability benchmark (0–100 km/h in 9.9 s).

Topology	Motor size (kW)		Transmission ratio		Battery capacity (kW h)	Energy consumption (kW h/100 km)	Powertrain cost (US\$)
	Front	Rear	Front	Rear			
Case study	80	—	7.9	—	24.0	16.5 ($\pm 0.0\%$)	8900
SM-SA	80	—	8.1	—	23.0	16.4 (-0.5%)	8600
DM-DA	42	46	6.56	6.29	24.0	16.4 (-0.3%)	9400
IWM-SA	2 \times 43	—	Direct drive		21.1	16.2 (-1.8%)	8500
IWM-DA	2 \times 29	2 \times 17	Direct drive		22.3	16.0 (-3.3%)	9800

SM-SA: single-motor single-axle; DM-DA: double-motor double-axle; IWM-SA: in-wheel-motor single-axle; IWM-DA: in-wheel-motor double-axle.

Table 7. Powertrain cost for each topology after optimisation, subject to a constraint of meeting a specified energy consumption benchmark (16.45 kW h/100 km).

Topology	Motor size (kW)		Transmission ratio		Battery capacity (kW h)	Powertrain cost (US\$)	Acceleration time for 0–100 km/h (s)
	Front	Rear	Front	Rear			
Case study	80	—	7.9	—	24.0	8900 ($\pm 0.0\%$)	9.9
SM-SA	84	—	8.0	—	23.0	8700 (-2.4%)	9.3
DM-DA	60	40	8.0	8.0	24.0	9600 ($+8.0\%$)	8.0
IWM-SA	2 \times 62	—	Direct drive		20.5	9000 ($+0.9\%$)	7.0
IWM-DA	2 \times 65	2 \times 20	Direct drive		23.3	11,300 ($+26.0\%$)	6.0

SM-SA: single-motor single-axle; DM-DA: double-motor double-axle; IWM-SA: in-wheel-motor single-axle; IWM-DA: in-wheel-motor double-axle.

the topologies using in-wheel motors. Better acceleration naturally requires a large motor with a higher mass, which therefore consumes more energy. Table 6 shows the energy consumption at the benchmark acceleration. To meet this performance while minimising the energy efficiency, the Pareto-optimal solutions for every topology required a motor of at least 80 kW. The IWM-DA vehicle gives the best energy efficiency result with an improvement of more than 3% in comparison with the benchmark vehicle. The optimised SM-SA vehicle can be considered as the optimised form of the case-study vehicle. To obtain the same acceleration performance, the motor size remained the same, but the Pareto-optimal efficiency was achieved using a slightly larger gear ratio and a smaller battery than those of the original vehicle. This does not in any sense mean that the original-case-study vehicle was wrong; it is possible that the manufacturers had slightly different objectives in mind for their design process. If anything, it is reassuring for this methodology to find how close our optimal solution is to their design.

It is clear from this that, if obtaining a maximum efficiency for a given acceleration performance is required, then an in-wheel motor topology is the best choice. In particular, the best trade-off is obtained with the IWM-DA configuration. It should be noted, however, that this is also likely to be the most expensive powertrain.

So far, we have looked at the trade-offs between the energy consumption and the performance.

Figure 14 shows another trade-off: the energy consumption versus the powertrain cost. In this case, the

incumbent SM-SA topology gives the best trade-off curve, with the IWM-SA topology the second best. The lowest costs achievable relative to the energy consumption of the benchmark vehicle are shown in Table 7. The cheapest powertrain was achieved with a slightly larger motor (84 kW), a slightly larger gear ratio (8.9:1) and a slightly smaller battery size. The powertrain was 2.3% cheaper than that of the original-case-study vehicle. The other topologies produced more expensive vehicles, although the additional costs were not uniform; the IWM-SA vehicle was about 1% more expensive, while the IWM-DA vehicle was about 26% more expensive. There is a clear conflict here; the IWM-DA machine was the best in terms of the energy consumption versus the acceleration, but it is the worst in terms of the cost. The SM-SA vehicle is the cheapest for a given efficiency, but the worst performing. The IWM-SA vehicle gives a reasonable compromise between all three objectives. The costs and benefits of each topology can be summarised.

SM-SA

The SM-SA configuration has the simplest BEV powertrain, using a topology close to a traditional mechanical layout including a fixed-ratio gearbox and a large single power source. This has a low cost and is simple to control. The smallest motor size that can complete the complete CADC was 60 kW; this solution has a poor acceleration but consumes the minimum energy. This topology's greatest benefit is its low cost, but it does not give a good trade-off between the energy consumption and the performance.

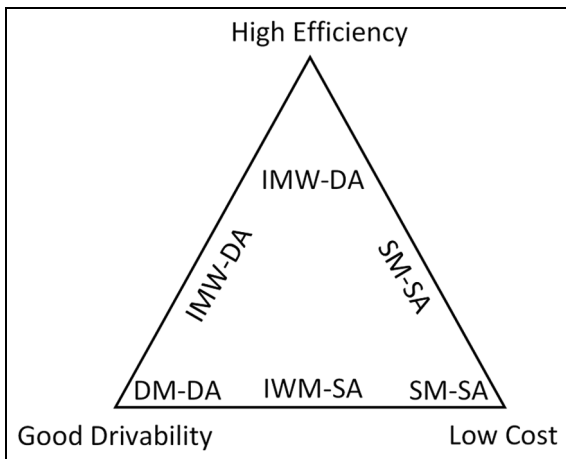


Figure 15. Trade-offs between different topologies and different objective functions. IWM-DA: in-wheel-motor double-axle; SM-SA: single-motor single-axle; DM-DA: double-motor double-axle; IWM-SA: in-wheel-motor, single-axle.

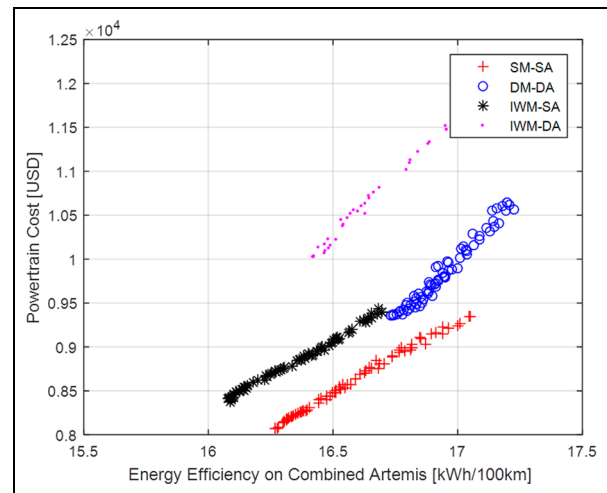


Figure 17. Pareto front of the energy consumption and the powertrain cost with the assumption of a full payload in the optimization. USD: US\$; SM-SA: single-motor single-axle; DM-DA: double-motor double-axle; IWM-SA: in-wheel-motor single-axle; IWM-DA: in-wheel-motor double-axle.

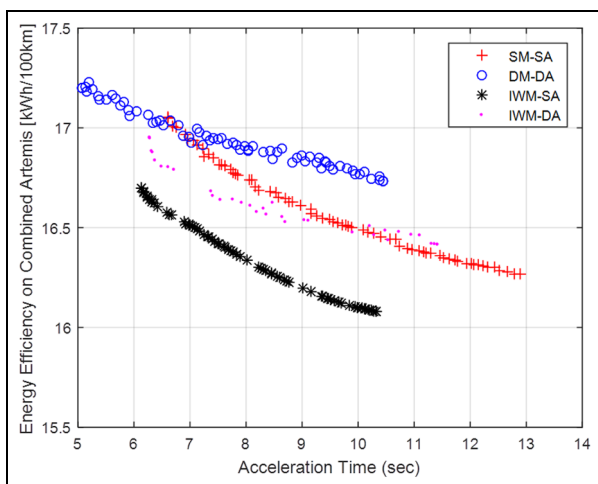


Figure 16. Pareto front of the acceleration time and the energy consumption with the assumption of a full payload in the optimization. SM-SA: single-motor single-axle; DM-DA: double-motor double-axle; IWM-SA: in-wheel-motor single-axle; IWM-DA: in-wheel-motor double-axle.

DM-DA

This BEV topology used two separate motors for the front axle and the rear axle. By allowing different motor sizings and different gear ratios at the front and the rear, it was possible to achieve an improved energy efficiency and acceleration performance in comparison with those of the baseline vehicle and the SM-SA vehicle. However, it was relatively expensive for any given energy consumption. It was much cheaper than the IWM-DA vehicle for a given acceleration. The DM-DA vehicle is most useful for a cheap performance car or four-wheel-drive vehicle. In both these scenarios, an IWM-DA vehicle gives a better performance but is

much more expensive; a DM-DA vehicle is reasonable and more affordable.

IWM-SA

The IWM-SA vehicle was slightly more expensive than the SM-SA vehicle. It was able to give a better energy consumption and a better acceleration performance. This is good for passenger cars that do not need a four-wheel drive for a very high performance. This topology may well be suitable for the future small city car. Complexity of control and consideration of electronic differential algorithms were not considered, and neither was the increased unsprung mass. These problems are likely to be surmountable with further work.

IWM-DA

The IWM-DA vehicle produced a good acceleration time with minimum energy consumption but was the most expensive topology. It is excellent for efficient performance vehicles, but it is expensive. Where four-wheel drive is not required, the IWM-SA vehicle can provide a better compromise between all three objectives.

Figure 15 gives guidelines on the selection of an appropriate topology to meet any given combination of objectives. For a general all-round vehicle, the IWM-SA and SM-SA topologies are likely to prove the best.

Robustness of solutions

In order to test the robustness of the solutions obtained, the optimisation was repeated, but a maximum payload of 395 kg was assumed for the vehicle. The results are shown in Figure 16 and Figure 17. It can be seen that the results changed significantly.

- For the compromise between the efficiency and the driveability, the IWM-SA topology is the best choice. The IWM-DA topology is the second best.
- For the compromise between the efficiency and the powertrain cost, the SM-SA vehicle is still significant.
- For the compromise between the driveability and the cost, the IWM-SA vehicle is still a good choice but is not significantly different from the SM-SA vehicle.

Whether these results should take precedence over the results for the unladen vehicle depends very much on the way that car manufacturers interpret consumer desires.

Conclusions

In this paper a study was presented in which the properties of four possible BEV topologies were studied. The topologies used different combinations of in-body and in-wheel motors, driving axles and powertrain arrangements. The background to the topologies was presented, and four topologies selected for detailed analysis were described: SM-SA, DM-DA, IWM-SA and IWM-DA. These were modelled, and the calculations and the assumptions that we used were presented. The results of the models were presented, first showing how each topology performed with a fixed 80 kW total motor power, and then after performing multi-objective optimisation. The relative benefits of each topology were evaluated and presented, with guidelines on the choice of topology for given objectives. For pure energy efficiency or a good compromise between the energy efficiency and the driving performance, the IWM-DA topology was the best; for pure driving performance, the DM-DA topology was the best; for a cheap vehicle or a good compromise between the cost and the efficiency, the SM-S A topology was the best; for a cheap vehicle with a good performance, the IWM-SA topology was the best. Also, there was a significant sensitivity of the result to the problem formulation, as shown by the addition of a full payload to the vehicle. It is hoped that these guidelines and the method used to obtain them are useful for vehicle manufacturers in determining the best topologies to consider in the design of future BEVs.

Future work

There are a number of potential avenues for future investigation.

1. The impact of driverless cars on powertrain configuration should be considered. At present, powertrain sizing is constrained by a need to provide user-friendly driveability properties. Broadly, this requires powertrains to be sized for high torque capabilities, which perhaps are not strictly needed for satisfactory progression. A planned study will

consider a self-driving urban vehicle (perhaps a future taxi) in order to understand the distinctive aspects of optimisation of such a powertrain.

2. The techniques used in this study can be applied to evaluate the powertrains best suited to non-traditional power sources (such as lithium–sulphur batteries), or for non-passenger (i.e. freight) road transport applications. The fundamental principles here will not be different, but the duty cycles and the relative importance of some of the vehicle properties will change dramatically.
3. The metrics so far were the powertrain cost, the efficiency and the performance. There is a growing body of work that considers the relationship between the usage and the component lifespan. It will be valuable to investigate this relationship in future work.

Acknowledgment

Pongpun Othaganont thanks the Ministry of Science & Technology, Thailand, for the funding that supported this work.

Funding

The author(s) received no financial support for the research, authorship, and/or publication of this article.

Declaration of conflicting interests

The author(s) declared no potential conflicts of interest with respect to the research, authorship, and/or publication of this article.

References

1. European Commission. Environment, Transport emissions, Air pollutants from road transport, <http://ec.europa.eu/environment/air/transport/road.htm> (2014, accessed 27 August 2014).
2. [UK] Department for Transport. Policy, Transport emissions, <https://www.gov.uk/government/publications/plug-in-car-grant>, Plug-in car grant (2014, accessed 27 August, 2014).
3. Guzzella L and Sciarretta A. *Vehicle propulsion systems: introduction to modeling and optimization*. Berlin: Springer, 2005.
4. Dextreit C, Assadian F, Kolmanovsky V et al. Hybrid electric vehicle energy management using game theory. SAE paper 2008-01-1317, 2008.
5. Dextreit C and Kolmanovsky V. Game theory controller for hybrid electric vehicles. *IEEE Trans Control Systems Technol* 2014; 22(2): 652–663.
6. Weissinger C, Buecherl D and Herzog H. Conceptual design of a pure electric vehicle. In: *2010 IEEE vehicle power and propulsion conference*, Lille, France, 1–3 September 2010, pp. 1–5. New York: IEEE.
7. Hayes JG, Oliveria RPR, Vaughan S and Egan MG. Simplified electric vehicle power train models and range estimation. In: *2011 IEEE vehicle power and propulsion conference*, Chicago, Illinois, USA, 6–9 September 2011, pp. 1–5. New York: IEEE.

8. Pearre NS, Kempton W, Guensler RL and Elango V. Electric vehicles: how much range is required for a day's driving? *Transpn Res Part C: Emerging Technol* 2011; 19(6): 1171–1184.
9. Ehsani M, Gao Y and Emadi A. *Modern electric, hybrid electric, and fuel cell vehicles: fundamentals, theory, and design*. 2nd edition. Boca Raton, Florida: CRC Press, 2009, p. 557.
10. Guiron Z, Henghai Z and Houyu L. The driving control of pure electric vehicle. *Procedia Environ Sci* 2011; 10(A): 433–438.
11. Wang R, Chen Y, Feng D et al. Development and performance characterization of an electric ground vehicle with independently actuated in-wheel motors. *J Power Sources* 2011; 196(8): 3962–3971.
12. Lightning Car Company. A new way of motoring, <http://www.lightningcarcompany.co.uk> (2014, accessed 27 August 2014).
13. van Schalkwyk DJ and Kamper MJ. Effect of hub motor mass on stability and comfort of electric vehicles. In: *2006 IEEE vehicle power and propulsion conference*, Windsor, Ontario, Canada, 6–8 September 2006, pp. 1–6. New York: IEEE.
14. Jain M and Williamson SS. Suitability analysis of in-wheel motor direct drives for electric and hybrid electric vehicles. In: *2009 IEEE electrical power and energy conference*, Montreal, Quebec, Canada, 22–23 October 2009, pp. 1–5. New York: IEEE.
15. Yan X and Patterson D. Improvement of drive range, acceleration and deceleration performance in an electric vehicle propulsion system. In: *30th annual IEEE power electronics specialists conference*, Charleston, South Carolina, USA, 1 July 1999, Vol 2, pp. 638–643. New York: IEEE.
16. Benysek G and Jarnut M. Electric vehicle charging infrastructure in Poland. *Renewable Sustainable Energy Rev* 2012; 16(1): 320–328.
17. Zhou B, Jiang Q, Yang Y and Wang J. Analysis of energy consumption and powertrain parameters optimization of BEV based on running cycle. In: *2010 IEEE 11th international conference on computer-aided industrial design and conceptual design*, Yiwu, Zhejiang, People's Republic of China, 17–19 November 2010, pp. 1284–1290. New York: IEEE.
18. Hu X, Murgovski N, Johannesson LM and Egardt B. Optimal dimensioning and power management of a fuel cell/battery hybrid bus via convex programming. *IEEE/ASME Trans Mechatronics* 2016; 20(1): 457–468.
19. Othaganont P, Assadian F and Auger D. Sensitivity analyses for cross-coupled parameters in automotive powertrain optimization. *Energies* 2014; 7(6): 3733–3747.
20. Wipke KB, Cuddy MR and Burch SD. ADVISOR 2.1: a user-friendly advanced powertrain simulation using a combined backward/forward approach. *IEEE Trans Veh Technol* 1999; 48(6): 1751–1761.
21. Mohan G, Assadian F and Longo S. Comparative analysis of forward-facing models vs backward-facing models in powertrain component sizing. In: *2013 4th IET hybrid and electric vehicles conference*, London, UK, 6–7 November 2013, pp. 1–6. New York: IEEE.
22. Yang Y, Hu X, Pei H and Peng Z. Comparison of power-split and parallel hybrid powertrain architectures with a single electric machine: dynamic programming approach. *Appl Energy* 2016; 168: 683–690.
23. Mohan G, Assadian F and Longo S. An optimization framework for comparative analysis of multiple vehicle powertrains. *Energies* 2013; 6: 5507–5537.
24. Leitman S and Brant B. *Build your own electric vehicle*. 2nd edition. New York: McGraw-Hill, 2009.
25. Larminie J and Lowry J. *Electric vehicle technology explained*. Chichester, West Sussex: John Wiley, 2004.
26. Chen GH and Tseng KJ. Design of a permanent-magnet direct-driven wheel motor drive for electric vehicle. In: *27th annual IEEE power electronics specialists conference*, Baveno, Italy, 23–27 June 1996, Vol 2, pp. 1933–1939. New York: IEEE.
27. Qian H, Xu G, Yan Q et al. Energy management for four-wheel independent driving vehicle. In: *2010 IEEE/RSJ international conference on intelligent robots and systems*, Taipei, Republic of China, 18–22 October 2010, pp. 5532–5537. New York: IEEE.
28. Tesla Motors. Home page, <http://www.teslamotors.com> (2014, accessed 27 August 2014).
29. Caricchi F, Crescimbeni F, Di Napoli A and Marchegiani M. Prototype of electric vehicle drive with twin water-cooled wheel direct drive motors. In: *27th annual IEEE power electronics specialists conference*, Baveno, Italy, 23–27 June 1996, Vol 2, pp. 1926–1932. New York: IEEE.
30. Qian H, Lam TL, Li W et al. System and design of an omni-directional vehicle. In: *IEEE international conference on robotics and biomimetics*, Bangkok, Thailand, 21–26 February 2008, pp. 389–394. New York: IEEE.
31. Rahman KM, Patel NR, Ward TG et al. Application of direct-drive wheel motor for fuel cell electric and hybrid electric vehicle propulsion system. *IEEE Trans Ind Appl* 2006; 42(5): 1185–1192.
32. Tao G, Ma Z, Zhou L and Li L. A novel driving and control system for direct-wheel-driven electric vehicle. In: *2004 12th symposium on electromagnetic launch technology*, Snowbird, Utah, USA, 25–28 May 2004, pp. 514–517. New York: IEEE.
33. Yang Y-P and Hu T-H. A new energy management system of directly-driven electric vehicle with electronic gear-shift and regenerative braking. In: *2007 American control conference*, New York, USA, 9–13 July 2007, pp. 4419–4424. New York: IEEE.
34. Tie SF and Tan CW. A review of energy sources and energy management system in electric vehicles. *Renewable Sustainable Energy Rev* 2013; 20: 82–102.
35. Dejun Y and Hori Y. A novel traction control of EV based on maximum effective torque. In: *IEEE 2008 vehicle power and propulsion conference*, Harbin, Heilongjiang, People's Republic of China, 3–5 September 2008, pp. 1–6. New York: IEEE.
36. Hori Y. Future vehicle driven by electricity and control-research on four wheel motored “UOT Electric March II”. In: *2002 7th international workshop on advanced motion control*, Maribor, Slovenia, 3–5 July 2002, pp. 1–14. New York: IEEE.

37. Sakai S, Sado H and Hori Y. Motion control in an electric vehicle with four independently driven in-wheel motors. *IEEE/ASME Trans Mechatronics* 1999; 4(1): 9–16.
38. Wang J, Wang Q, Jin L and Song C. Independent wheel torque control of 4WD electric vehicle for differential drive assisted steering. *Mechatronics* 2011; 21(1): 63–76.
39. Sorniootti A, Boscolo M, Turner A and Cavallino C. Optimization of a multi-speed electric axle as a function of the electric motor properties. In: *2010 IEEE vehicle power and propulsion conference*, Lille, France, 1–3 September 2010, pp. 1–6. New York: IEEE.
40. Lukic SM and Emado A. Modeling of electric machines for automotive applications using efficiency maps. In: *Electrical insulation conference and electrical manufacturing coil winding technology conference*, Indianapolis, Indiana, USA, 23–25 September 2003, pp. 543–550. New York: IEEE.
41. Sato Y, Ishikawa S, Okubo T et al. Development of high response motor and inverter system for the Nissan LEAF electric vehicle. SAE paper 2011-01-0350, 2011.
42. Protean Electric. In-wheel motor, torque-speed characteristics. Company website, www.proteanelectric.com/specifications (2015, accessed 7 July 2015).
43. YASA. In-wheel motor torque–speed characteristics, <http://www.yasamotors.com/products> (2015, accessed 7 July 2015).
44. Simpson A. Cost–benefit analysis of plug-in hybrid electric vehicle technology. In: *22nd international battery, hybrid and fuel cell electric vehicle symposium and exhibition*, Yokohama, Japan, 22–28 October 2006, paper NREL/CP-540-40485. Golden, Colorado: National Renewable Energy Laboratory.
45. Nissan Motor Co. EV/HEV safety, LEAF battery specifications, www.nhtsa.gov/pdf/ev/Nissan_Presentation-Bob_Yakushi.pptx (2012, accessed 7 July 2015).
46. The MathWorks, Inc. *Global Optimization Toolbox R2014a user's guide*. Natick, Massachusetts The MathWorks, Inc., 2014, section 5.3.
47. Othaganont P, Assadian F and Marco J. Battery electric vehicle powertrain simulation to optimise range and performance'. In: *International conference on powertrain modelling and control*, Bradford, West Yorkshire, UK, 4–6 September 2012. The University of Bradford School of Engineering, Design and Technology.

G_R	rear gear ratio in a double-axle vehicle (dimensionless)
$I_{T,bat}$	current from the battery terminals (A)
$J_i(X_D)$	objective (cost) function i parameterized on the decision variables X_D (units vary)
M	mass of the vehicle (kg)
M_x	mass of the component x (kg)
$P_{in,total}$	total machine input power (W)
P_M	electric machine power (W)
$P_{out,total}$	total machine output power (W)
Q	instantaneous charge of the battery (C)
Q_{bat}	capacity of the battery (C)
Q_{init}	initial instantaneous charge of the battery (C)
$R_{i,bat}$	internal resistance of the battery pack (Ω)
$R_{i,cell}$	internal resistance of a single cell (Ω)
r_w	radius of a wheel (m)
t	time (s)
T_F	torque at the front axle in a double-axle vehicle (N m)
T_M	torque at the machine axle (N m)
T_R	torque at the rear axle in a double-axle vehicle (N m)
T_S	torque split between the front machine and the rear machine (dimensionless)
T_{SB}	torque split during braking (dimensionless)
T_w	torque at the wheel axle (N m)
T_{100}	time taken to accelerate from rest to 100 km/h (s)
$v_{vehicle}$	speed of the vehicle (m/s)
$V_{OCV,bat}$	open-circuit voltage of a complete battery pack (V)
$V_{OCV,cell}$	open-circuit voltage of a single cell (V)
$V_{T,bat}$	voltage at the battery terminals (V)
$V_{T,cell}$	voltage at a single cell (V)
η_F	efficiency of the front electric machine in a double-axle vehicle (rad/s)
η_G	efficiency of the gearbox (dimensionless)
η_M	efficiency of the electric machine (dimensionless)
η_R	efficiency of the electric machine in a double-axle vehicle (rad/s)
ρ	density of air (kg/m^3)
ϕ_F	power rating of the front machine in a double-axle vehicle (kW)
ϕ_M	power rating of the electric machine (kW)
ϕ_R	power rating of the rear machine in a double-axle vehicle (kW)
ω_M	angular velocity of the electric machine (rad/s)
$\omega_{M,front}$	angular velocity of the front machine in a double-axle vehicle (rad/s)
$\omega_{M,rear}$	angular velocity of the rear machine in a double-axle vehicle (rad/s)
ω_w	angular velocity of the wheels (rad/s)

Appendix I

Notation

A	vehicle drag area (m^2)
C_d	drag coefficient (dimensionless)
C_r	coefficient of rolling resistance (dimensionless)
E	energy required to complete a specified driving cycle (J)
$f(x)$	function of the variable x (units vary)
f_w	driving force at the wheels (N)
g	acceleration due to gravity (m/s^2)
G_F	front gear ratio in a double-axle vehicle (dimensionless)

Abbreviations

BEV	battery electric vehicle	IWM-DA	in-wheel-motor double-(driven-)axle
CADC	Common Artemis Driving Cycle	IWM-SA	in-wheel motor single-(driven-)axle
GA	genetic algorithm	NEDC	New European Driving Cycle
HEV	hybrid electric vehicle	SOC	state of charge (dimensionless)
ICE	internal-combustion engine	DM-DA	double-motor double-(driven-)axle
		SM-SA	single-motor single-(driven-)axle